ACS Macro Letters
Letter
Cite This: ACS Macro Lett. 2019, 8, 84−87
pubs.acs.org/macroletters

All-DNA System Close to the Percolation Threshold

J. Fernandez-Castanon,*[,†] M. Zanatta,[‡] L. Comez,[§] A. Paciaroni,[∥] A. Radulescu,[⊥] and F. Sciortino[†,#]

[†]Sapienza−Università di Roma, P.le A. Moro 5, 00185 Rome, Italy
[‡]Dipartimento di Informatica, Università di Verona, 37134 Verona, Italy
[§]CNR-IOM c/o Dipartimento di Fisica e Geologia, Università degli Studi di Perugia, 06123 Perugia, Italy
[∥]Dipartimento di Fisica e Geologia, Università di Perugia, 06123 Perugia, Italy
[⊥]Jülich Centre for Neutron Science (JCNS) at Heinz Maier-Leibnitz Zentrum (MLZ), Forschungszentrum Jülich GmbH, 85748 Garching, Germany
[#]CNR-ISC, UOS Sapienza−Università di Roma, 00185 Rome, Italy

Supporting Information

ABSTRACT: We characterize via small-angle neutron scattering the structural properties of a mixture of all-DNA particles with functionalities 4 (A) and 2 (B) constrained by design to reside close to the percolation threshold. DNA base sequences are selected such that A particles can only bind with B ones and that at the studied temperature (10 °C) all AB bonds are formed and long-lived, originating highly polydisperse persistent equilibrium clusters. The concentration dependence of the scattered intensity and its wavevector dependence is exploited to determine the fractal dimension and the size distribution of the clusters, which are found to be consistent with the critical exponents of the 3-D percolation universality class. The value of DNA nanoparticles as nanometric patchy colloids with well-defined functionality, bonding selectivity, and exquisite control of the interaction strength is demonstrated.

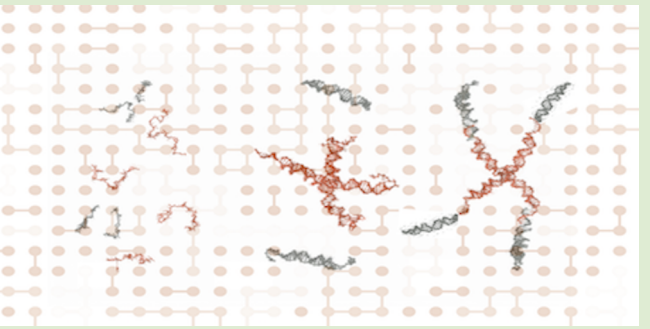

Binary mixtures of particles with different functionality restricted by chemical design to form only bonds between monomers of different type have been proposed in the field of polyfunctional condensation as an example of systems in which percolation can be approached by tuning the relative concentration.[1,2] Indeed the maximum number of formed bonds is automatically fixed by the number of reactive sites of the minority species.[3] A powerful application of this idea lies at the heart of vitrimers, modern plastics characterized by dynamically reconfigurable networks.[4,5] In soft-gel systems, this approach has been recently exploited by Li and co-workers[6] in their study of two different tetra-armed PEG polymers in which the chemical bonding between the two species is controlled by maleimide and thiol reactive end groups.

In this letter, we report a neutron investigation of an all-DNA binary mixture programmed to reside in thermal equilibrium close to the percolation threshold. Both types of particles (A and B), differing in their functionality, are created by combining suitably selected DNA sequences and decorated with sticky ends to exclusively permit the formation of AB bonds. We thus rely on the flexibility offered by DNA as a material molecule[7,8] to build self-assembled all-DNA particles with precise dimension, shape, and functionality and, at the same time, to control the interparticle interactions via the sticky ends. Exploiting DNA self-assembly, we generate bulk quantities of identical particles, which allow us to study their collective behavior in a thermally reversible controllable way. In the last years, these particles have been used as model systems to experimentally test[9−11] interesting predictions resulting from theoretical and numerical studies based on the physics of patchy colloids[12,13] and to investigate self-assembling in liquid crystals[14−16] and other interesting aggregation phenomena in soft matter.[17−19]

A pictorial representation of the selected particles and of the self-assembly process is reported in Figure 1 and discussed in detail in Sections II and III of the SI. Such a process, starting from isolated strands, generates first particles with functionality 4 (A) and 2 (B), and then their clustering. Since AA or BB links are forbidden, B particles act as bridges joining the nodes (the A particles) of a tetrafunctional network. In this DNA system, the number of interparticle bonds and their lifetime can be precisely controlled, in a completely reversible way, by tuning temperature (T), as previous rheological,[20] DLS,[9,10,21] and SANS[22] investigations of gelling DNA nanostars have demonstrated. With sticky ends composed by eight bases, the lifetime of the AB bonds becomes longer than hundreds of minutes at T = 10 °C, providing a controlled physical system in thermal

Received: October 26, 2018
Accepted: December 27, 2018

DOI: 10.1021/acsmacrolett.8b00822
ACS Macro Lett. 2019, 8, 84−87

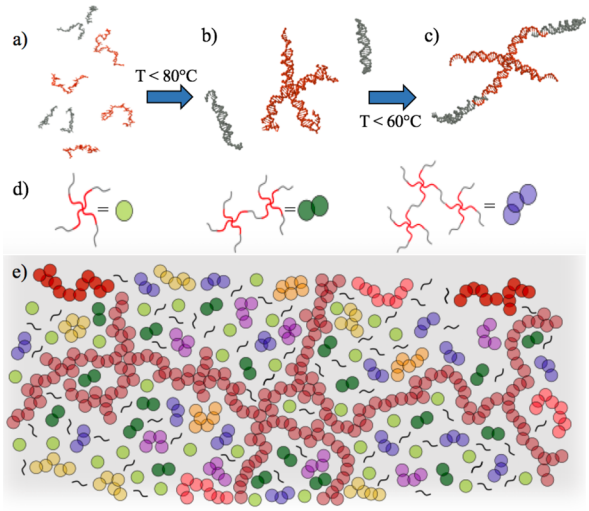

Figure 1. Self-assembling process of the A and B structures (see Sections II and III of the SI for further details). It starts (a) from complementary DNA single strands. Four distinct single strands pair below ≈80 °C to form A structures (red) and two to form each B unit (gray) as shown in (b). By further lowering T below ≈60 °C, binding via the complementary sticky ends starts to take place, resulting in the formation of AB bonds. Panel (c) shows one A particle coordinated with two B ones. Panel (d) displays the three smallest AB clusters: AB_4 (left), A_2B_7 (center), and A_3B_{10} (right). Since there is an excess of B particles compared to the stoichiometric composition, all A sticky ends are bonded. In (d) each one of the AB_4 structures is also depicted as one circle, in preparation of the drawing in panel (e). A sketch representing the state of the system for composition $x \approx 0.14$ is shown in (e). Here, clusters with similar sizes are labeled with identical colors. The dark red cluster indicates a cluster that spans the whole system. Gray lines indicate B particles in excess that are not bonded to any A units.

equilibrium that mimics the chemical analogue on the experimental observation time scale. On varying the relative concentration of A and B particles, it is possible to tune the structure of the system. When there are two B for each A, the stoichiometric ratio, the system forms at low T a fully bonded structure in which all particles are part of the network. On increasing the relative concentration of B particles, while all sticky ends of the A particles remain bonded, some of the B sticky ends, now in excess, rest unpaired, and the network progressively increases the number of dangling ends. For a critical value of the relative concentration, the system reaches the percolation threshold.[23] At this critical point, the spanning cluster disappears, and the system becomes composed by an extremely polydisperse solution of finite size clusters.[24]

In this article, we focus via small-angle neutron scattering (SANS) on the structural properties of this all-DNA AB system at the composition $x = 0.14$, close to the percolation threshold (here $x \equiv N_A/(N_A + N_B)$ where N_A (N_B) indicates the number of A (B) particles). Keeping the relative composition fixed, we measure the scattered intensity by progressively diluting the system with buffer down to the limit where cluster−cluster interactions are negligible. The choice of $x = 0.14$ has been based on the mean-field predictions,[23,25] indicating that percolation is expected at $x = 1/7 \approx 0.14$, i.e., when there are approximately six B particles for each A. A preliminary characterization[26] via dynamic light scattering of the system for different x values confirms that indeed at $x = 0.14$ the correlation function decays following a logarithmic t dependence, a signature of proximity to a percolation transition. Technical details about the neutron experiment and on sample preparation are reported in Section I of the SI.

The evolution of the scattered intensity on dilution and its wavevector dependence is exploited to determine the fractal dimension and the size distribution of the clusters, which are found to be consistent with the critical exponents of the 3-D percolation universality class.

Figure 2 displays the measured scattering intensities $I(q)$ multiplied by the dilution factor ϕ (to account for the trivial concentration dependence) for different values of ϕ. A dashed magenta line at $q \approx 0.1$ Å^{-1} divides a region of high q values, where the scattering intensity is essentially independent of the sample concentration and a low q region where the intensities depend on ϕ. The $q \approx 0.1$ Å^{-1} value corresponds to distances of about 60 Å in real space, a figure that should be compared with the linear dimension of the particle arms. Hence, in this q window the scattered intensity essentially reflects the structure of the double helix composing A and B. The smaller q region shows instead a clear increase in the scattered intensity on dilution, suggesting a significant role arising from cluster−cluster interactions, physically originating from excluded volume and electrostatic repulsion of the negatively charged DNA phosphate groups. This ϕ-dependent signal will be used in the following to quantify the percolating structure of the system. Here, we stress that although the temperature is the factor responsible for controlling the DNA NS aggregation the cluster−cluster interaction is entirely dependent on the number of DNA NSs per unit volume, i.e., the DNA concentration.

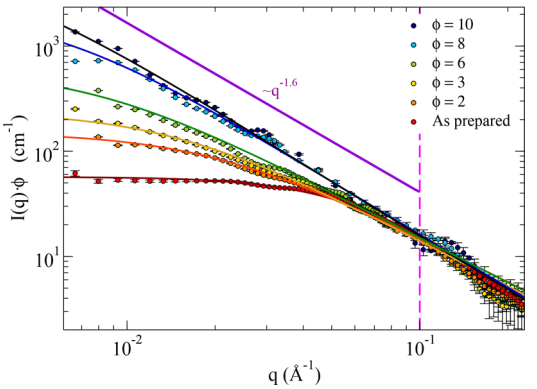

Figure 2. SANS measurements for a sample with total particle concentration (both A and B particles) ≈ 398 μM (labeled as "as prepared") and for the same sample after different dilution factors ϕ. The magenta line indicates $q = 0.1$ Å^{-1}. Solid lines represent the best fitting of the experimental data according to eq 1. The corresponding fit parameters are shown in Figure 3. A line with slope $q^{-d_{eff}}$, with $d_{eff} = 1.6$ (as theoretically expected for percolation of diluted swollen branched polymer chains[27]), is also shown.

Since it is not possible to provide an accurate description of the cluster−cluster interactions in such a polydisperse case, several approximated functions have been proposed in the past to model the q dependence of the scattered intensity close to percolation. To interpolate between an Ornstein−Zernike-like expression ruling the response at small q and a power-law function reflecting the self-similar nature of the system ($(q)^{-d_{eff}}$) at intermediate q we select the functional form

$$I(q) = \frac{I(0)}{1 + h(q)(q\xi)^2} \quad (1)$$

DOI: 10.1021/acsmacrolett.8b00822
ACS Macro Lett. 2019, 8, 84−87

where

$$h(q) = \frac{1}{1 + (q\xi)^{2-d_{\mathrm{eff}}}} \quad (2)$$

This functional form interpolates between two known limits: $I(0)[1\text{-}q^2\xi^2]$ at small q and a fractal $q^{-d_{\mathrm{eff}}}$ at large q. It thus provides a minimum parameter functional form with the expected limiting behaviors to describe the unifying scaling properties of solutions of self-similar clusters. This function was originally proposed in ref 28 in the context of semidilute solutions of polymer chains and recently selected in a SANS study of PEG mixtures of tetravalent stars.[6] In eq 1, $I(0)$ indicates the scattered intensity at $q = 0$ and ξ, the spatial correlation length, originating from intra- and intercluster terms. The intracluster term does not change with ϕ since the polydispersity of the sample is fixed, being encoded in the choice of x. The length scale associated with the intracluster term (also indicated as connectivity length) diverges at percolation due to the presence of clusters at the verge of spanning the entire sample volume. The intercluster contribution, which vanishes at infinite dilution, is known to suppress correlation.[29,30] For this reason, the correlation length ξ is expected to decrease on decreasing ϕ. The term d_{eff} corresponds to the effective fractal dimension of the clusters, an exponent which includes information both on the cluster fractal dimension d_f and on the system self-similar polydispersity, as discussed in more detail below.

The solid lines in Figure 2 (resulting from a best-fit of the region $q < 0.1$ Å^{-1}) show that eq 1 properly describes the data. The associated fitting parameters $I(0)$ and ξ and their ϕ dependence are shown in Figure 3(a) and (b), respectively.

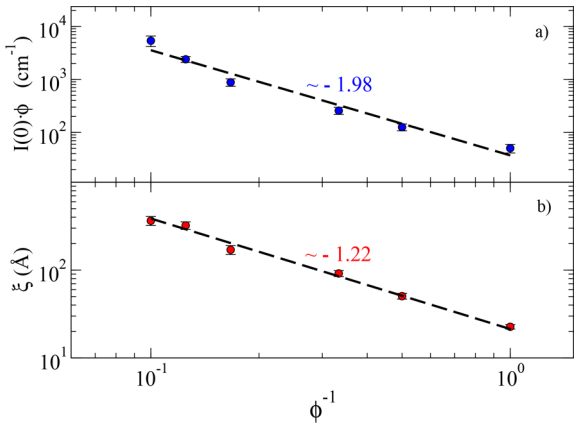

Figure 3. (a) $I(0)\phi$ values from the fitting of each curve of Figure 2 according to eq 1 as a function of ϕ^{-1}. Note that we present the data as a function of ϕ^{-1} being ϕ^{-1} proportional to the particle concentration. The dashed line corresponds to the best fit according to a power-law in ϕ, resulting in $I(0)\phi \sim \phi^{1.98}$. (b) Estimated ξ values extracted from the fit according to eq 1. The power-law best fit to these points is shown as a dashed line, from which $\xi \sim \phi^{1.22}$.

Interestingly, both quantities are consistent with a power-law relationship with best-fit exponents −1.98 and −1.22, respectively. The last fit parameter in eq 1 is the effective fractal dimension d_{eff}. For all different dilutions, the same value $d_{\mathrm{eff}} = 1.61 \pm 0.02$ properly represents the data. As described by eq 1, the region of wavevectors where the self-similar scaling $I(q) \sim q^{-d_{\mathrm{eff}}}$ is detectable increases on increasing ϕ, as clearly shown by the data in Figure 2.

To explain the origin of the difference between d_{eff} and d_f, it is necessary to consider the large polydispersity that characterizes a system close to percolation. In the region of wavelengths where the fractal structure is sampled, the scattering intensity of a single fractal object is expected to scale as[31] $I \sim q^{-d_f}$. In the case of systems close to percolation, the cluster size distribution becomes itself self-similar, an effect quantified by the Fisher exponent τ. The cluster size distribution N_s, i.e., the number of clusters of size s, indeed behaves as $N_s \sim s^{-\tau}$. Following the expressions derived by Martin and Ackerson[32] and Bouchad et al.,[27] the combination of the self-similar scattering of individual clusters and the self-similar behavior of the polydispersity results in $I \sim q^{-(3-\tau)d_f}$. Hence

$$d_{\mathrm{eff}} = (3 - \tau)d_f \quad (3)$$

Assuming the universal 3D percolation value for $\tau = 2.18$,[33] the experimental data suggest that $d_f = 1.96$. Interestingly, such a value is very close to two, the value which has been predicted and measured for percolation of swollen branched polymer chains.[27,34]

In summary, we have investigated via SANS the structure of an all-DNA mixture of tetravalent and bivalent particles close to its percolation transition, emphasizing the importance of using SANS to characterize the self-assembly of DNA nanostructures. The DNA sticky-end sequences have been designed in such a way that the only possible association process involves particles of different type (AB bonding). Similarly, the number of bases in the sticky-end sequence has been selected in such a way that at the experimentally studied T (10 °C) all possible bonds in the system are formed at all densities.[35] As shown in the SI, the SantaLucia thermodynamic model suggests that complete AB bonding takes place already at 35 °C. In addition, DLS measurements[26] have been performed to support and confirm the SantaLucia calculations.[36,37] Finally, the relative concentration of the two particle types has been selected in such a way that, when all possible bonds are formed, the system is close to the percolation threshold. Thus, this study shows the exquisite control that it is possible to achieve working with DNA nanoparticles and the efficiency of the self-assembling mechanisms that lead to the formation of a complex system entirely made by DNA. We have here demonstrated how it is possible to design a DNA system which, by self-assembly, locates itself, in thermal equilibrium, close to the percolation threshold, developing a self-similar distribution of fractal clusters, in full agreement with theoretical expectations. Such a system, besides offering an exquisitely controllable colloidal analogue of molecular polyfunctional condensation, could provide the appropriate model for experimentally testing the theoretically proposed extension of the critical Casimir forces[38] to the percolating case.[39] We expect these results will stimulate future investigations in further exploiting the unlimited possibilities offered by DNA nanoparticles as model systems[9,10] as well as building blocks of smart materials (e.g., DNA-plastics) with innovative and tunable properties.

■ ASSOCIATED CONTENT

Supporting Information

The Supporting Information is available free of charge on the ACS Publications website at DOI: 10.1021/acsmacrolett.8b00822.

Technical details of SANS experiments, system design and sample preparation methods, and theoretical

DOI: 10.1021/acsmacrolett.8b00822
ACS Macro Lett. 2019, 8, 84−87

calculations of the melting profiles of the DNA system under different dilution conditions (PDF)

AUTHOR INFORMATION

Corresponding Author

*E-mail: javi.fernandez.castanon@gmail.com.

ORCID

J. Fernandez-Castanon: 0000-0002-9994-8461

L. Comez: 0000-0001-5160-6844

Notes

The authors declare no competing financial interest.

ACKNOWLEDGMENTS

F.S. and J.F.C. acknowledge support from ETN-COLLDENSE (H2020-MCSA-ITN-2014, Grant No. 642774) and Regione Lazio (Grant No. 85857-0051-0085). Authors thank L. Rovigatti for providing the designs presented in Figure 1(a−c).

REFERENCES

(1) Rubinstein, M.; Colby, R. H. *Polymer Physics*; Oxford University Press: New York, 2003; Vol. *23*.

(2) Tanaka, F. *Polymer Physics: Applications to Molecular Association and Thermoreversible Gelation*; Cambridge University Press, 2011.

(3) Stockmayer, W. H. Molecular distribution in condensation polymers. *J. Polym. Sci.* **1952**, *9* (9), 69.

(4) Montarnal, D.; Capelot, M.; Tournilhac, F.; Leibler, L. Silica-like malleable materials from permanent organic networks. *Science* **2011**, *334*, 965−968.

(5) Capelot, M.; Unterlass, M. M.; Tournilhac, F.; Leibler, L. Catalytic control of the vitrimer glass transition. *ACS Macro Lett.* **2012**, *1*, 789−792.

(6) Li, X.; Hirosawa, K.; Sakai, T.; Gilbert, E. P.; Shibayama, M. SANS Study on Critical Polymer Clusters of Tetra-Functional Polymers. *Macromolecules* **2017**, *50*, 3655.

(7) Seeman, N. C. DNA nanotechnology: novel DNA constructions. *Annu. Rev. Biophys. Biomol. Struct.* **1998**, *27*, 225.

(8) Seeman, N. C. DNA in a material world. *Nature* **2003**, *421*, 427.

(9) Biffi, S.; Cerbino, R.; Bomboi, F.; Paraboschi, E. M.; Asselta, R.; Sciortino, F.; Bellini, T. Phase behavior and critical activated dynamics of limited-valence DNA nanostars. *Proc. Natl. Acad. Sci. U. S. A.* **2013**, *110*, 15633.

(10) Bomboi, F.; Romano, F.; Leo, M.; Fernandez-Castanon, J.; Cerbino, R.; Bellini, T.; Bordi, F.; Filetici, P.; Sciortino, F. Re-entrant DNA gels. *Nat. Commun.* **2016**, *7*, 13191.

(11) Salamonczyk, M.; Zhang, J.; Portale, G.; Zhu, C.; Kentzinger, E.; Gleeson, J. T.; Jakli, A.; De Michele, C.; Dhont, J. K.; Sprunt, S.; Stiakakis, E. Smectic phase in suspensions of gapped DNA duplexes. *Nat. Commun.* **2016**, *7*, 13358.

(12) Bianchi, E.; Largo, J.; Tartaglia, P.; Zaccarelli, E.; Sciortino, F. Phase diagram of patchy colloids: Towards empty liquids. *Phys. Rev. Lett.* **2006**, *97*, 168301.

(13) Roldán-Vargas, S.; Smallenburg, F.; Kob, W.; Sciortino, F. Gelling by heating. *Sci. Rep.* **2013**, DOI: 10.1038/srep02451.

(14) Nakata, M.; Zanchetta, G.; Chapman, B. D.; Jones, C. D.; Cross, J. O.; Pindak, R.; Bellini, T.; Clark, N. A. End-to-end stacking and liquid crystal condensation of 6−to 20−base pair DNA duplexes. *Science* **2007**, *318*, 1276−1279.

(15) Zanchetta, G.; Nakata, M.; Buscaglia, M.; Bellini, T.; Clark, N. A. Phase separation and liquid crystallization of complementary sequences in mixtures of nanoDNA oligomers. *Proc. Natl. Acad. Sci. U. S. A.* **2008**, *105*, 1111−1117.

(16) Siavashpouri, M.; Wachauf, C. H.; Zakhary, M. J.; Praetorius, F.; Dietz, H.; Dogic, Z. Molecular engineering of chiral colloidal liquid crystals using DNA origami. *Nat. Mater.* **2017**, *16*, 849.

(17) Li, Y.; Tseng, Y. D.; Kwon, S. Y.; d'Espaux, L.; Bunch, J. S.; McEuen, P. L.; Luo, D. Controlled assembly of dendrimer-like DNA. *Nat. Mater.* **2004**, *3*, 38.

(18) Jochum, C.; Adžić, N.; Stiakakis, E.; Derrien, T. L.; Luo, D.; Kahl, G.; Likos, C. N. Structure and stimuli-responsiveness of all-DNA dendrimers: theory and experiment. *Nanoscale* **2019**, DOI: 10.1039/C8NR05814H.

(19) Brady, R. A.; Brooks, N. J.; Cicuta, P.; Di Michele, L. Crystallization of amphiphilic DNA C-stars. *Nano Lett.* **2017**, *17*, 3276−3281.

(20) Fernandez-Castanon, J.; Bianchi, S.; Saglimbeni, F.; Di Leonardo, R.; Sciortino, F. Microrheology of DNA Hydrogels Gelling and Melting On Cooling. *Soft Matter* **2018**, *14*, 6431.

(21) Bomboi, F.; Biffi, S.; Cerbino, R.; Bellini, T.; Bordi, F.; Sciortino, F. *Eur. Phys. J. E: Soft Matter Biol. Phys.* **2015**, *38*, 1−8.

(22) Fernandez-Castanon, J.; Bomboi, F.; Rovigatti, L.; Zanatta, M.; Paciaroni, A.; Comez, L.; Porcar, L.; Jafta, C. J.; Fadda, G. C.; Bellini, T.; Sciortino, F. Small-angle neutron scattering and molecular dynamics structural study of gelling DNA nanostars. *J. Chem. Phys.* **2016**, *145*, No. 084910.

(23) Stockmayer, W. H. Theory of molecular size distribution and gel formation in branched-chain polymers. *J. Chem. Phys.* **1943**, *11*, 45.

(24) Stauffer, D. Scaling theory of percolation clusters. *Phys. Rep.* **1979**, *54*, 1−74.

(25) Flory, P. J. Molecular size distribution in three dimensional polymers. i. gelation. *J. Am. Chem. Soc.* **1941**, *63*, 3083.

(26) Fernandez-Castanon, J.; Bomboi, F.; Sciortino, F. Binding branched and linear DNA structures: From isolated clusters to fully bonded gel. *J. Chem. Phys.* **2018**, *148*, No. 025103.

(27) Bouchaud, E.; Delsanti, M.; Adam, M.; Daoud, M.; Durand, D. Gelation and percolation: swelling effect. *J. Phys. (Paris)* **1986**, *47*, 1273−1277.

(28) Bastide, J.; Candau, S. J. In *The Physical Properties of Polymer Gels - Ch. 9*; Cohen Addad, J. P., Ed.; 143; John Wiley: New York, 1996.

(29) Coniglio, A.; Stanley, H. E.; Klein, W. Site-bond correlatedpercolation problem: a statistical mechanical model of polymer gelation. *Phys. Rev. Lett.* **1979**, *42*, 518.

(30) Adam, M.; Delsanti, M.; Durand, D.; Hild, G.; Munch, J. Mechanical properties near gelation threshold, comparison with classical and 3D percolation theories. *Pure Appl. Chem.* **1981**, *53*, 1489−1494.

(31) Teixeira, J. Small-angle scattering by fractal systems. *J. Appl. Crystallogr.* **1988**, *21*, 781−785.

(32) Martin, J. E.; Ackerson, B. J. Static and dynamic scattering from fractals. *Phys. Rev. A: At., Mol., Opt. Phys.* **1985**, *31*, 1180.

(33) Paul, G.; Ziff, R. M.; Stanley, H. E. Percolation threshold, Fisher exponent, and shortest path exponent for four and five dimensions. *Phys. Rev. E: Stat. Phys., Plasmas, Fluids, Relat. Interdiscip. Top.* **2001**, *64*, No. 026115.

(34) Stauffer, D.; Aharony, A. *Introduction to percolation theory*; revised second ed.; CRC press, 2014.

(35) Zadeh, J. N.; Steenberg, C. D.; Bois, J. S.; Wolfe, B. R.; Pierce, M. B.; Khan, A. R.; Dirks, R. M.; Pierce, N. A. NUPACK: analysis and design of nucleic acid systems. *J. Comput. Chem.* **2011**, *32*, 170−173.

(36) SantaLucia, J. A unified view of polymer, dumbbell, and oligonucleotide DNA nearest-neighbor thermodynamics. *Proc. Natl. Acad. Sci. U. S. A.* **1998**, *95*, 1460−1465.

(37) SantaLucia, J., Jr; Hicks, D. The thermodynamics of DNA structural motifs. *Annu. Rev. Biophys. Biomol. Struct.* **2004**, *33*, 415−440.

(38) Hertlein, C.; Helden, L.; Gambassi, A.; Dietrich, S.; Bechinger, C. Direct measurement of critical Casimir forces. *Nature* **2008**, *451*, 172.

(39) Gnan, N.; Zaccarelli, E.; Sciortino, F. Casimir-like forces at the percolation transition. *Nat. Commun.* **2014**, *5*, 3267.

DOI: 10.1021/acsmacrolett.8b00822
ACS Macro Lett. 2019, 8, 84−87